

NASA  
Technical  
Memorandum

NASA TM - 103540

THE CORROSION PROTECTION OF 2219-T87  
ALUMINUM BY ANODIZING

By M.D. Danford

Materials and Processes Laboratory  
Science and Engineering Directorate

June 1991

(NASA-TM-103540) THE CORROSION PROTECTION  
OF 2219-T87 ALUMINUM BY ANODIZING (NASA)  
50 1 CSCL 11F

NO1-26312

Unclass

65/26 0025627



National Aeronautics and  
Space Administration

George C. Marshall Space Flight Center



1. Report No. <b>NASA TM - 103540</b>		2. Government Accession No.		3. Recipient's Catalog No.	
4. Title and Subtitle <b>The Corrosion Protection of 2219-T87 Aluminum by Anodizing</b>				5. Report Date <b>June 1991</b>	
				6. Performing Organization Code	
7. Author(s) <b>M.D. Danford</b>				8. Performing Organization Report No.	
				10. Work Unit No.	
9. Performing Organization Name and Address <b>George C. Marshall Space Flight Center Marshall Space Flight Center, Alabama 35812</b>				11. Contract or Grant No.	
				13. Type of Report and Period Covered <b>Technical Memorandum</b>	
12. Sponsoring Agency Name and Address <b>National Aeronautics and Space Administration Washington, DC 20546</b>				14. Sponsoring Agency Code <b>NASA</b>	
15. Supplementary Notes  <b>Prepared by Materials and Processes Laboratory, Science and Engineering Directorate.</b>					
16. Abstract  <p>Various types of anodized coatings have been studied for 2219-T87 aluminum. These include both type II and type III anodize coats which have been water sealed and a newly developed and proprietary Magnaplate HCR™ coat. Results indicate that type III anodizing is not much superior to type II anodizing as far as corrosion protection for 2219-T87 aluminum is concerned. Magnaplate HCR™ coatings should provide superior corrosion protection over an extended period of time using a coating thickness of 51 microns (2.0 mils).</p>					
17. Key Words (Suggested by Author(s)) <b>2219-T87 aluminum, corrosion protection by anodizing, ac impedance spectroscopy, comparison of anodizing types in corrosion protection</b>				18. Distribution Statement  <b>Unclassified – Unlimited Subject Category: 26</b>	
19. Security Classif. (of this report) <b>Unclassified</b>		20. Security Classif. (of this page) <b>Unclassified</b>		21. No. of pages <b>30</b>	
				22. Price <b>NTIS</b>	



## **ACKNOWLEDGMENT**

The author wishes to thank Dr. C.P. Covino of the General Magnaplate Corporation for supplying specimens coated with Magnaplate HCR™.



## TABLE OF CONTENTS

	Page
INTRODUCTION.....	1
THE AC IMPEDANCE METHOD.....	2
EXPERIMENTAL.....	3
RESULTS AND DISCUSSION.....	4
A Comparison of Type II and Type III Anodizing.....	4
A Comparison of Type II Anodizing at High and Low pH.....	5
The Corrosion of Magnaplate-Coated Samples at High and Low pH.....	6
A Comparison of the Magnaplate Coating With Other Coating Types.....	7
CONCLUSIONS.....	7
REFERENCES.....	8

## LIST OF ILLUSTRATIONS

Figure	Title	Page
1.	Primary equivalent circuit model for analysis of ac impedance data.....	11
2.	Equivalent circuit model for calculating the Warburg coefficient.....	12
3.	Exploded view of the sample holder.....	13
4.	Magnified view of anodized 2219-T87 aluminum.....	14
5.	Magnified view of anodized 6061-T6 aluminum.....	14
6.	Magnified view of Magnaplate HCR™ coating.....	15
7.	Highly magnified view of Magnaplate HCR™ coating showing tiny cracks.....	15
8.	$R(T)$ , $R(P)$ , and Warburg coefficient-time curves for type II anodizing.....	16
9.	$I_{CORR}$ , water fraction, and delamination-time curves for type II anodizing.....	17
10.	$R(T)$ , $R(P)$ , and Warburg coefficient-time curves for type III anodizing.....	18
11.	$I_{CORR}$ , water fraction, and delamination-time curves for type III anodizing.....	19
12.	$R(T)$ , $R(P)$ , and $I_{CORR}$ -time curves for type II anodizing at pH 5.3.....	20
13.	$R(T)$ , $R(P)$ , and $I_{CORR}$ -time curves for type II anodizing at pH 8.8 .....	21
14.	$R(T)$ , $R(P)$ , and $I_{CORR}$ -time curves for Magnaplate HCR™ coat at pH 5.5.....	22
15.	$R(T)$ , $R(P)$ , and $I_{CORR}$ -time curves for Magnaplate HCR™ coat at pH 8.9.....	23



## LIST OF TABLES

Table	Title	Page
1.	Chemistry of 2219-T97 aluminum.....	9
2.	Comparison of average corrosion rates for type II and type III anodizing.....	9
3.	Comparison of average corrosion rates for type II anodizing and Magnaplate at high and low pH.....	10
4.	Comparison of average corrosion rates for various anodized aluminum samples at high and low pH.....	10



## TECHNICAL MEMORANDUM

# THE CORROSION PROTECTION OF 2219-T87 ALUMINUM BY ANODIZING

## INTRODUCTION

Aluminum alloy 2219-T87 is used extensively in the construction of both the external tank and the solid rocket booster skirts of the space shuttle system because of its high strength at cryogenic and elevated temperatures, resistance to stress corrosion cracking, and good weldability. It is also being seriously considered as the baseline material for construction of the space station element modules. However, it is subject to general corrosion and to pitting corrosion when exposed to a humid environment, and especially to an environment containing chloride ions.

Coatings being considered for corrosion protection are anodized surfaces (both type II and type III), epoxy primer, and primer-topcoat systems. Decisions concerning the use of these protective coatings will have to be made after considering the degree of corrosion protection required. It is generally believed that type III or hard-anodized surfaces give superior corrosion protection than do surfaces with the type II or conventional sulfuric acid anodized coatings. However, type III anodizing is difficult to perform in the case of 2219-T87 aluminum because of the alloy's high copper content (6.3 percent). In this study, an attempt was made to compare the corrosion protection of both types of anodizing. A good epoxy primer coat will very probably give better corrosion protection than either of the anodized surface treatments, although conditions may not be such that the painted surfaces are required. In addition, a study was made of Magnaplate HCR™,<sup>1</sup> a high-technology synergistic coating which produces a harder-than-steel surface and should exhibit extraordinarily improved corrosion resistance over hard anodized aluminum. An aluminum alloy of unspecified composition and temper, coated with a 51-micron (2.0-mil) coat of Magnaplate HCR™, showed little or no effects of corrosion after 24 months of continuous exposure to the atmosphere and to a 5-percent salt spray in tests performed by other laboratories. However, the high copper content of 2219-T87 aluminum is a factor to be considered.

All measurements in this work were performed with ac impedance spectroscopy, and utilized the dc polarization resistance technique where possible. Comparisons of corrosion resistance were made at both high and low pH for several types of anodized aluminum alloys. While it is believed that the results of this study are both accurate and reproducible, it must be stated that the achievement of properly anodized surfaces for the small sample disks employed in this work is very difficult because the current and voltage requirements used in the anodizing process are generally set up for much larger specimens.

## THE AC IMPEDANCE METHOD

The primary equivalent circuit model used for analysis of the ac impedance data is shown in figure 1. The circuit model of figure 2 was used to calculate the effect of diffusion polarization. A contribution due to the Warburg impedance, or the effect due to diffusion polarization, is given by

$$Z_W = \sigma W^{-1/2} - j\sigma W^{-1/2} . \quad (1)$$

Here,  $Z_W$  is the Warburg impedance,  $W = 2\pi X$  frequency,  $j = \sqrt{-1}$ , and  $\sigma$  is the Warburg coefficient. The value of  $\sigma$  is obtained using the model of figure 2, and, generally, the higher the value of  $\sigma$ , the less is the diffusion of the surrounding medium through the specimen coat. If the value of  $\sigma$  exceeds that of the charge transfer parameter  $R_T$ , the corrosion is diffusion controlled. Trends in the  $\sigma$ -time curves usually correlate well with positions of maxima and minima in the  $I_{\text{CORR}}$ -time curves, where  $I_{\text{CORR}}$  is the corrosion current, and with trends in  $R_P$ -time curves, where  $R_P$  is the coating or pore resistance. The development and selection of these models has been discussed previously.<sup>2</sup>

Values for each of the circuit components in either figure 1 or figure 2 were treated as parameters in the nonlinear ORGLS<sup>3</sup> least-squares program, which automatically adjusted these parameters to obtain a best fit to the observed Bode magnitude data (log impedance versus log  $W$ ). Corrosion currents were calculated from ac impedance data using the relation

$$I_{\text{CORR}} = \frac{(b_a) \times (b_c)}{2.303 (b_a + b_c)} \cdot \frac{1}{R_T + R_R} , \quad (2)$$

which is the Stern-Geary equation for charge transfer control.<sup>4-6</sup> Tafel constants ( $b_a$  and  $b_c$ ) were assumed to be 50 mV each, and  $(R_T + R_R)$  is the total charge transfer resistance. The value of 50 mV each for the Tafel constants has been found to provide excellent agreement with values of  $I_{\text{CORR}}$  obtained by dc polarization resistance of measurements.<sup>7</sup> However, in cases where measurements using the polarization resistance technique were possible, values of  $I_{\text{CORR}}$  obtained with this technique were used because Tafel constants are calculated directly from the data and no assumptions are necessary. This was the situation for most of the measurements in the present work. The corrosion rate for 2219-T87 aluminum is given by

$$\text{Corrosion rate (mpy)} = 0.44014 \times I_{\text{CORR}} . \quad (3)$$

In some cases, two recently developed techniques were tried. One of these involved the calculation of water content in the coating.<sup>8</sup> The volume fraction of water is given by

$$C_c(t)/C_c(0) = 80^V, \quad (4)$$

where  $C_c(t)$  is the coating capacitance at time  $t$  and  $C_c(0)$  is the initial coating capacitance. This expression holds for low-volume fractions,  $V$ . The other technique involves the calculation of a delamination factor.<sup>9</sup> It is related to the impedance parameters by

$$S/S_0 = 2\pi f_h C_c R_p, \quad (5)$$

where  $S/S_0$  is fraction of surface area delaminated,  $f_h$  is the value of the frequency at which the phase shift is  $45^\circ$ ,  $C_c$  is the coating capacitance, and  $R_p$  is the pore resistance.  $S/S_0$  was determined only on a relative basis in this work, and only the trends in the  $S/S_0$  versus time curves were examined.

## EXPERIMENTAL

Magnaplate coated samples are prepared by a proprietary procedure and were supplied by the General Magnaplate Corporation. Although specimens, both 16 microns (0.625 mils) and 51 microns (2.0 mils) in coating thickness, are currently being tested in a 5-percent salt spray cabinet, results for the electrochemical methods are reported here. The salt spray test, a conventional method, will require a much longer period of time. Only the 16-micron coating thickness was studied in the present work. Disks of 2219-T87 aluminum, 1.43 cm (9/16 in) in diameter and 0.16 cm (1/16 in) thick, were anodized in-house using conventional sulfuric acid anodize, type II class 1, and hard anodized, type III class 1. Specimens were water-sealed in both cases. Attempts to hard anodize the small 1.43-cm diameter disks resulted in the burning of many of the disks; therefore, 10- by 15-cm (4- by 6-in) plates were hard anodized and disks stamped out afterwards. This procedure produced some crevice corrosion of the disks in the sample holder of the electrochemical cell (fig. 3), resulting from damage to the disk edges in the stamping process. As a result, in the case where type II anodizing was to be compared with type III anodizing, the type II anodizing was carried out by the same procedure. The small type II anodized disks were stamped out prior to anodizing where comparisons with the type III anodize were not carried out. In these cases, no crevice corrosion occurred.

Sample surfaces were wiped with alcohol to remove fingerprints. For comparison of the type II and type III coatings, samples were immersed in 3.5-percent sodium chloride (NaCl) solutions for 27 days, buffered at pH 8.2. Both the type II anodized and Magnaplate coated disks were placed in 3.5-percent NaCl solutions buffered at both a pH of about 5.5 and a pH of 8.9 in order to compare their behavior at high and low pH. Buffer solutions were

prepared as described previously.<sup>10</sup> A saturated calomel reference electrode was used in all electrochemical measurements.

Alternate current and dc polarization resistance measurements (where possible) were made on alternate days for the entire test period. The EG&G-PARC model 378 ac impedance system was used for the ac impedance measurements. These data were taken in three sections. The first two sections, beginning at 0.001 Hz and 0.1 Hz, respectively, were obtained using the fast Fourier transform technique. The last section, ranging from 6.28 to 40,000 Hz was collected using the lock-in amplifier technique. The sequencing was performed automatically using the autoexecute procedure, with all data merged to a single set for each run. The period of collection for the ac impedance data was approximately 3 hours. After collection, the data were processed and analyzed with the IBM PC/AT computer using the models shown in figures 1 and 2. This computer also controlled the experiment.

Data for the polarization resistance method were collected using the same instrumentation with the EG&G-PARC model 342C software, which was developed especially for dc measurements. The instrumentation developed by EG&G-PARC automatically corrected the data for IR drop during the scan. The data were analyzed using the program POLCURR.<sup>11</sup> The theory for the polarization resistance technique has been described previously.<sup>12</sup>

## **RESULTS AND DISCUSSION**

The chemistry of the 2219-T87 aluminum used in this work is presented in table 1. Magnified views of the surfaces of anodized 2219-T87 and 6061-T6 aluminum surfaces are compared in figures 4 and 5. The surfaces appear smoother in the case of 2219-T87 aluminum than for the 6061-T6 specimen. The craters which appear on the surface do not extend to the aluminum metal surface, as evidenced by cross sections of the samples. A magnified view of the Magnaplate surface, taken at  $\times 100$ , is shown in figure 6. A highly magnified view ( $\times 3,500$ ) of the Magnaplate surface is shown in figure 7 and reveals a tiny crack which is present in the surface. The depth of crack penetration is not known, but it probably does not extend to the aluminum metal surface.

### **A Comparison of Type II and Type III Anodizing**

Type III anodizing resulted in the burning of several of the small 1.43-cm diameter disks. Additional plates (10 by 15 cm) were anodized and the disks stamped subsequently. For comparative purposes, the same procedure was used for type II anodizing. This procedure resulted in damage to the edges of the disks, and some crevice corrosion was evident after exposure to salt water. Because of this, results are somewhat influenced by the crevice corrosion contribution, and corrosion rates are somewhat higher than they would be otherwise. Coating thicknesses were 8 microns (0.3 mils) for the type II anodizing and 10 microns (0.4 mils) for the type III anodizing. Curves obtained by ac impedance methods are shown in figures 8 and 9 for type II anodizing and in figures 10 and 11 for type III anodizing.

The charge transfer parameter  $R(T)$  (fig. 8A) for type II anodizing drops rather rapidly and reaches a minimum plateau after 4 days of exposure.  $R(P)$  (fig. 8B) starts at a relatively low value, rises somewhat, and drops rather slowly. The Warburg coefficient (fig. 8C) peaks at about 7 days and oscillates thereafter. The value of  $I_{CORR}$  (fig. 9A) ranges from about  $0.05 \mu\text{A}/\text{cm}^2$  to  $0.22 \mu\text{A}/\text{cm}^2$  at 27 days. The curve oscillates with time, generally characteristic of aluminum alloy corrosion. The curve for the volume fraction of water (fig. 9B) reaches a maximum at about 8 days and shows a gradual rise thereafter. The curve for the delamination parameter (fig. 9C) peaks at about 6 days and drops slowly. The curves for the charge transfer resistance  $R(T)$  and coating or pore resistance  $R(P)$  indicate poorer corrosion protection for type II anodizing than might be expected. Part of this is no doubt due to the crevice corrosion which occurred. The average corrosion rates over 7 and 27 day periods are shown in table 2 for type II anodizing. For the first 7 days of exposure, the average corrosion rate was 0.0285 mils/year (mpy) and was 0.0517 mpy for the 27-day period. For comparison, the corrosion rate of bare 2217-T87 aluminum was measured as 0.80 mpy.

In the case of type III anodizing, the curve for charge transfer resistance  $R(T)$  (fig. 10A) starts a value comparable to that for type II anodizing, but holds up over a longer time before reaching its minimal value. The coating resistance  $R(P)$  (fig. 10B) starts at a higher value than that for type II anodizing and remains higher throughout. Thus, the protective coating is somewhat better in this case. The Warburg coefficient (fig. 10C) peaks at 4 days, then drops and oscillates. The curve for  $I_{CORR}$  (fig. 11A) starts at  $0.005 \mu\text{A}/\text{cm}^2$  and peaks at  $0.22 \mu\text{A}/\text{cm}^2$  at 15 days.

The average corrosion rate was 0.0181 mpy for the first 7 days and 0.0343 mpy for the 27-day period. The average corrosion rates for type III anodizing are therefore about half those for type II anodizing. These values, of course, include the crevice corrosion. The results are summarized in table 2 for type II and type III anodizing.

The curve for the volume fraction of water (fig. 11B) remains at small values until it rises rather rapidly at about 18 days. The curve for the delamination parameter (fig. 11C) exhibits similar behavior. Trends in the curves for volume fraction of water and the delamination parameter correlate rather well with trends in the  $I_{CORR}$ -time curve in this case. In general, type III or hard anodizing provides only slightly better corrosion protection than the conventional type II sulfuric acid anodizing.

### **A Comparison of Type II Anodizing at High and Low pH**

All disks were stamped out prior to anodizing in this case, and the disks were individually anodized. Samples were compared by exposure to a 3.5-percent NaCl solution buffered at pH 5.3 and pH 8.8. The coating thickness was 5 microns (0.2 mils) in both cases. In these tests, no crevice corrosion was evident. Curves for samples exposed at pH 5.3 are shown in figure 12, while those for pH 8.8 are shown in figure 13.

The charge transfer resistance  $R(T)$  (fig. 12A) at pH 5.3 starts at about 1,000 k $\Omega$ , drops rapidly, and reaches a minimum at about 4 days. It remains at a reasonably high level thereafter at 50 to 100 k $\Omega$ . The coating resistance  $R(P)$  (fig. 12B) starts at 13.5 k $\Omega$  and declines slowly thereafter, but maintains a relatively high level throughout. The  $I_{CORR}$  curve (fig. 12C) starts at a very small value, peaks at about 4 days, and rises slowly thereafter

with oscillation. The average corrosion rate was 0.0113 mpy for the first 7 days and 0.0256 mpy for the 27-day period.

The charge transfer curve at pH 8.8 (fig. 13A) starts at a very high level, 97,000 k $\Omega$ , and drops more slowly to its minimal value at 7 days. Values of  $R(T)$  drop to a lower value than did those at pH 5.3 during the latter part of the exposure. The pore or coating resistance  $R(P)$  (fig. 13B) starts at 11 k $\Omega$  and maintains a high level for about 10 days. It falls to about the same level as did the corresponding curve at pH 5.3 beyond 10 days. The  $I_{CORR}$  curve (fig. 13C) starts at very small values, but rises very rapidly with oscillation during the latter part of the test. The coverage corrosion rate for the first 7 days was 0.008 mpy, and was 0.0207 mpy for the entire 27-day period. These values are, therefore, approximately the same at pH 5.3 and pH 8.8. Magnified views of the sample surfaces showed one medium-sized but rather deep pit in the sample exposed at pH 5.3, while three smaller, less shallow pits were evident in the sample exposed at pH 8.8. This is in accord with experiments performed earlier<sup>13</sup> in which it was found that pit initiation occurs more readily at high pH with a greater tendency toward pit passivation, as evidenced by the small pit size.

### **The Corrosion of Magnaplate-Coated Samples at High and Low pH**

Magnaplate HCR coats with thickness of 15.2 to 16.5 microns (0.6 to 0.65 mils) were applied individually to 1.43-cm diameter disks after stamping. The charge transfer curve  $R(T)$  is shown in figure 14A for a specimen exposed at pH 5.5. The curve starts at a value of about 16,000 k $\Omega$ , but rises to values as high as 60,000 k $\Omega$  and falls to a minimal value of about 500 k $\Omega$  after 11 days. The high values of  $R(T)$  thus persist much longer in the case of Magnaplate than for the type II anodized specimens. The value of  $R(P)$  (fig. 14B) shows similar characteristics, starting at about 9 k $\Omega$ , falling to a minimum at 11 days of about 2.5 k $\Omega$  and maintaining that level throughout. The  $I_{CORR}$  curve in figure 14C shows very small values initially and rises to a peak at 11 days, the same point at which the  $R(T)$  and  $R(P)$  curves reach their minimum values. The average corrosion rate is only 0.0002 mpy for the first 7 days and only 0.0095 mpy for the entire 27 days.

The sample exposed at pH 8.9 did not hold up quite as well. The  $R(T)$  curve in figure 15A starts at about 31,000 k $\Omega$  but shows steady decline, reaching a minimal value at 9 days. The pore or coating resistance  $R(P)$  in figure 15B shows somewhat better characteristics, starting at a value of 6.5 k $\Omega$  and rising to a maximum value of 15 k $\Omega$  at 7 days. It reaches a minimal value of 1.5 k $\Omega$  at 11 days and continues to drop beyond that point. The  $I_{CORR}$  curve (fig. 15C) exhibits rather small values up to about 16 days but rises very abruptly, peaking at a value of 0.2  $\mu A/cm^2$  at 21 days. Corrosion thus occurred very rapidly toward the end of the test, causing a higher average corrosion rate for the 27-day period. The average corrosion rate for the first 7 days was only 0.0007 mpy, about the same as that at pH 5.5, but the rapid rise in the final test stage at pH 8.9 increased the average rate to 0.0196 mpy for the 27-day period.

It might be argued that the difference at pH 8.9 could be attributed to the individual coating of the small disks, but two other samples tried at this pH also showed signs of early deterioration. Therefore, according to this test, the Magnaplate coating holds up better at pH 5.5 than at pH 8.9. Average corrosion rates for both type II anodizing and Magnaplate coated samples are summarized in table 3. Examination of the Magnaplate specimens, under



magnification after exposure, revealed a small but rather deep pit in the sample exposed at pH 5.5. The sample exposed at pH 8.9 showed a broader, less shallow pit, probably a result of three or four smaller pits which were initiated, but coalesced with time into a single, broader pit. Pitting characteristics are therefore similar to those for type II anodizing.

### **A Comparison of the Magnaplate Coating With Other Coating Types**

A comparison of corrosion rates at low and high pH for various samples is made in table 4. Average corrosion rates for 2219-T87 aluminum with the type II anodized coat, 6061-T6 aluminum with type III anodized coat, and Tufram coated 6061-T6 aluminum are listed for 7- and 27-day durations. Values of coating thickness and pH levels are also given.

The Magnaplate coat is equal or superior to all other coating types at low pH, in spite of the fact that the coating thickness is less in many cases. At high pH, the Magnaplate coat is superior to type II anodize, but seems to be inferior to a thicker type III anodized coat on prolonged exposure. However, for shorter exposure times, the thinner Magnaplate coat provides about equal protection. It is also evidently inferior to a much thicker Tufram coat on prolonged exposure at high pH. Again, the Magnaplate coat is at least equal to the much thicker Tufram coat for shorter exposure times. Since the Magnaplate coat can be applied to a thickness of 51 microns (2.0 mils), a coating of this thickness should provide superior corrosion protection for a prolonged period of time for 2219-T87 aluminum.

### **CONCLUSIONS**

Type II anodizing is only slightly better than type III anodizing as far as corrosion protection is concerned. Samples with the type II anodizing behave equally well at low and high pH. Magnaplate HCR, which was included in this study, showed superior corrosion protection at low pH for an extended period of time. A sample exposed at high pH showed excellent corrosion protection over the short range, but deteriorated after long exposure. The Magnaplate coatings for this work had a nominal thickness of 16 microns (0.625 mils). However, since coating thicknesses of 51 microns (2.0 mils) can be applied, coats of such thickness should provide superior corrosion protection for extended periods of time.

Magnaplate with a coating thickness of 51 microns (2.0 mils) is therefore highly recommended for 2219-T87 aluminum. It not only affords excellent corrosion protection, but presents a very hard (about RC-70), wear resistant, and durable surface.

## REFERENCES

1. The General Magnaplate Corporation, Linden, New Jersey.
2. Danford, M.D.: NASA Technical Memorandum, NASA TM-100402, June 1990.
3. Busing, W.R., and Levy, H.A.: "A General Nonlinear Least Squares Program ORGLS," Oak Ridge National Laboratory, 1958.
4. Stern, M., and Geary, A.L.: Journal of the Electrochemical Society, vol. 102, 1955, p. 609.
5. Stern, M., and Geary, A.L.: Journal of the Electrochemical Society, vol. 104, 1957, p. 56.
6. Stern, M.: Corrosion, vol. 14, 1958, p. 440t.
7. Danford, M.D.: NASA Technical Memorandum, NASA TM-100366, April 1989.
8. Kendig, M., and Scully, J.: Corrosion, vol. 46, No. 1, January 1990, p. 22.
9. Haruyama, S., Asari, M., and Tsurw, T.: "Corrosion Protection by Organic Coatings." M. Kendig and H. Leidheiser (editors), Proceedings, vol. 87-2, Pennington, New Jersey, Electrochemical Society, 1987.
10. Danford, M.D.: NASA Technical Memorandum, NASA TM-100394, April 1990.
11. Gerchakov, S.M., Udey, L.R., and Mansfield, F.: "An Improved Method for Analysis of Polarization Resistance Data." Corrosion, vol. 37, 1981, p. 696.
12. Danford, M.D., and Higgins, R.H.: NASA Technical Paper 2459, April 1985.
13. Danford, M.D.: Memorandum EH24 (83-39), September 1983.

Table 1. Chemistry of 2219-T97 aluminum.

Element	Listed Weight Percent (ASTM B-209)	Measured Weight Percent (MSFC Analysis)
Silicon (Si)	0.2 Maximum	0.100
Copper (Cu)	5.8 – 6.8	6.700
Iron (Fe)	0.3 Maximum	0.227
Manganese (Mn)	0.2 – 0.4	0.220
Zinc (Zn)	0.1 Maximum	0.030
Titanium (Ti)	0.02 – 0.10	0.085
Vanadium (V)	0.05 – 0.15	0.092
Zirconium (Zr)	0.10 – 0.25	0.128
Chromium (Cr)	0.05 Maximum	0.024
Aluminum (Al)	Balance	92.394

Table 2. Comparison of average corrosion rates for type II and type III anodizing.

Coat	Seal	$\overline{CR}$ (7 Days) mpy	$\overline{CR}$ (27 Days) mpy	pH	State
Type II	Water	0.0285	0.0517	8.2	CC*
Type III	Water	0.0181	0.0343	8.2	CC*

\*Crevice corrosion occurred.

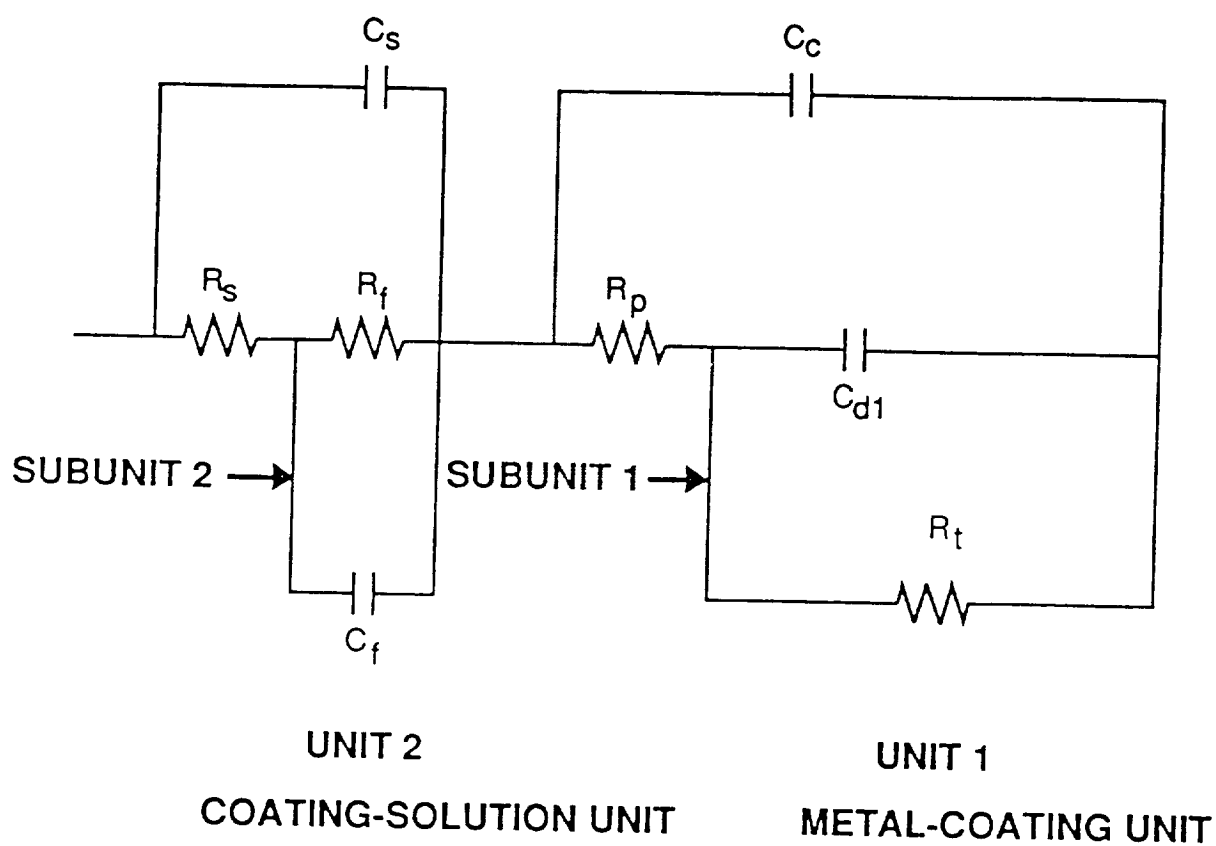
Table 3. Comparison of average corrosion rates for type II anodizing and Magnaplate at high and low pH.

Coat	Seal	$\overline{CR}$ (7 Days) mpy	$\overline{CR}$ (27 Days) mpy	pH
Type II	Water	0.0113	0.0256	5.3
Type II	Water	0.0008	0.0207	8.8
Magnaplate	—	0.0002	0.0095	5.5
Magnaplate	—	0.0007	0.0196	8.9

Table 4. Comparison of average corrosion rates for various anodized aluminum samples at high and low pH.

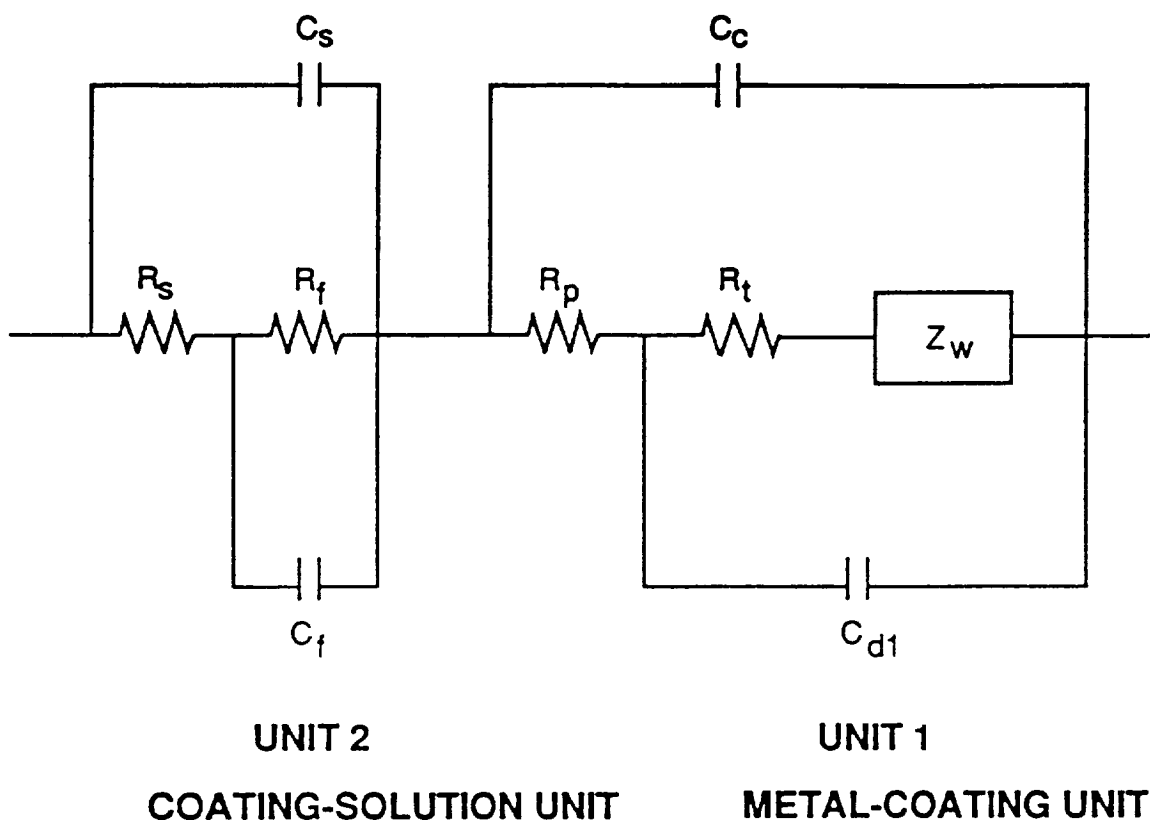
Coat	Type Aluminum	Coating Thickness Microns	$\overline{CR}$ (7 Days) mpy	$\overline{CR}$ (27 Days) mpy	pH
Type II	2219-T87 (H <sub>2</sub> O)*	05	0.0113	0.0256	5.3
Type II	2219-T87 (H <sub>2</sub> O)*	05	0.0008	0.0207	8.8
Type III	6061-T6 (H <sub>2</sub> O)*	25	0.0020	0.0041	5.5
Type III	6061-T6 (H <sub>2</sub> O)*	25	0.0004	0.0001	9.5
Tufram	6061-T6	40	0.0110	0.0171	5.5
Tufram	6061-T6	40	0.0014	0.0004	9.5
Magnaplate	2219-T87	16	0.0002	0.0095	5.5
Magnaplate	2219-T87	16	0.0007	0.0196	8.9

\*Water sealed.



- $C_s$  SOLUTION CAPACITANCE
- $R_s$  SOLUTION RESISTANCE
- $C_f$  FARADAIC CAPACITANCE (COATING/SOLUTION)
- $R_f$  FARADAIC RESISTANCE
- $C_c$  COATING CAPACITANCE
- $R_p$  COATING RESISTANCE
- $R_t$  CHARGE TRANSFER RESISTANCE
- $C_{d1}$  METAL/COATING INTERFACE CAPACITANCE

Figure 1. Primary equivalent circuit model for analysis of ac impedance data.



- $C_s$  SOLUTION CAPACITANCE
- $R_s$  SOLUTION RESISTANCE
- $C_f$  FARADAIC CAPACITANCE (COATING/SOLUTION)
- $R_f$  FARADAIC RESISTANCE
- $C_c$  COATING CAPACITANCE
- $R_p$  COATING RESISTANCE
- $R_t$  CHARGE TRANSFER RESISTANCE
- $C_{d1}$  METAL/COATING INTERFACE CAPACITANCE
- $Z_w$  WARBURG IMPEDANCE (DIFFUSION POLARIZATION)

Figure 2. Equivalent circuit model for calculating the Warburg coefficient.

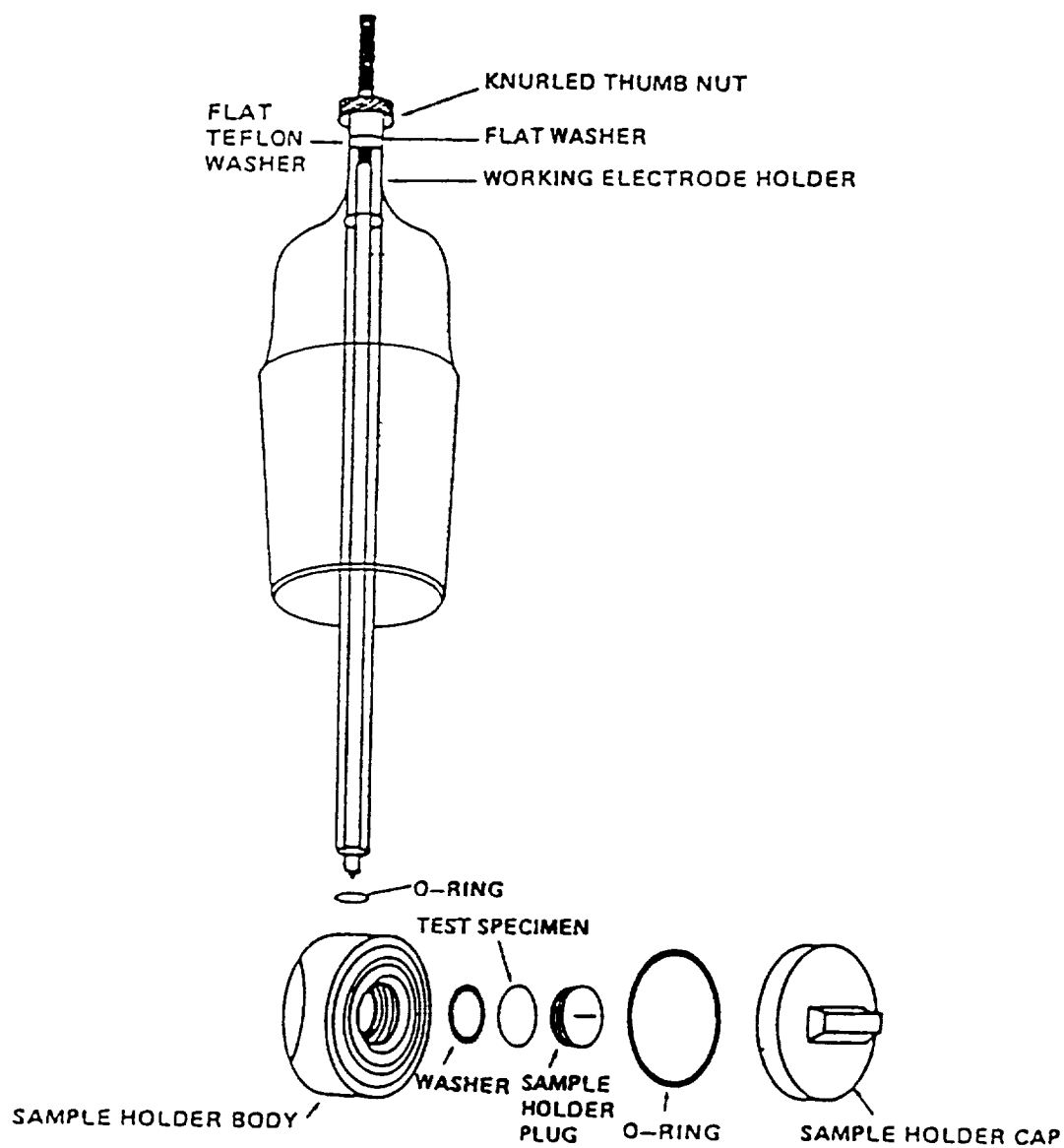


Figure 3. Exploded view of the sample holder.

ORIGINAL PAGE  
BLACK AND WHITE PHOTOGRAPH

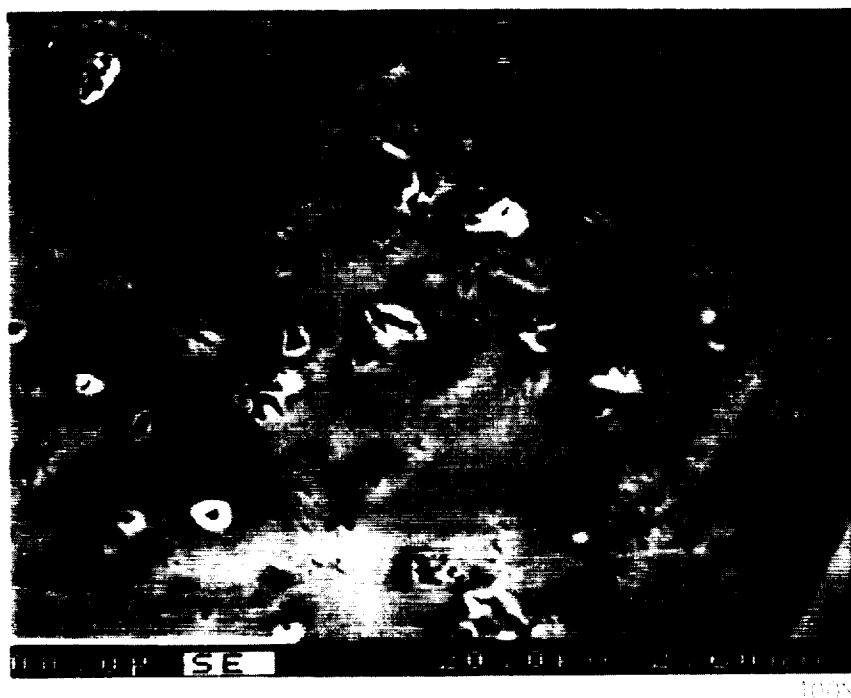


Figure 4. Magnified view of anodized 2219-T87 aluminum.

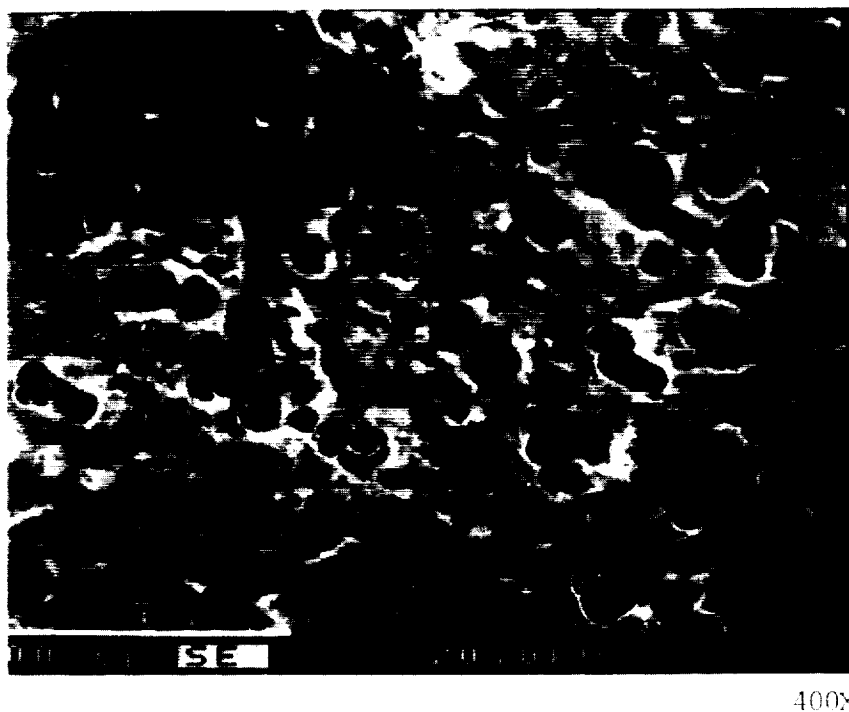


Figure 5. Magnified view of anodized 6061-T6 aluminum.



ORIGINAL FILE  
BLACK AND WHITE PHOTOGRAPH

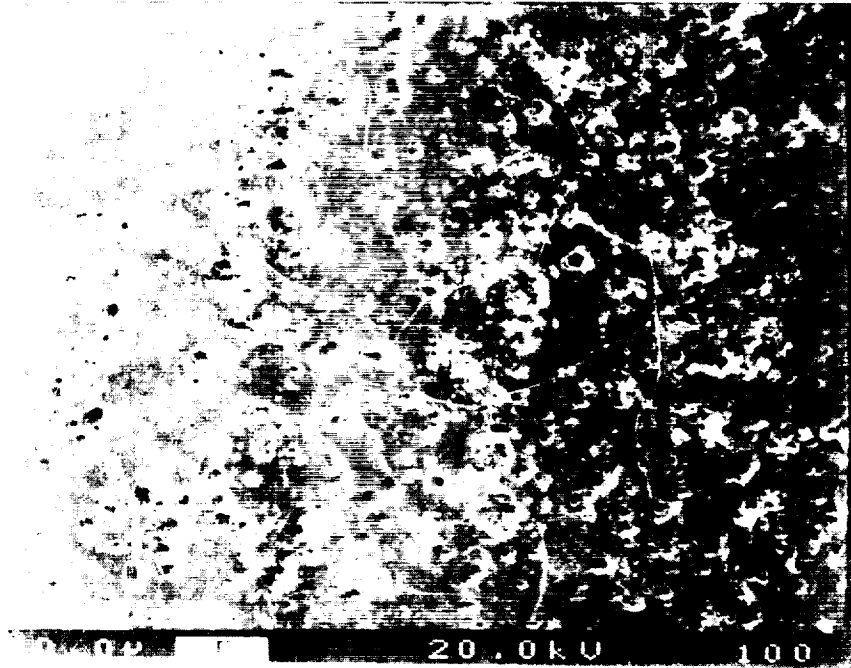


Figure 6. Magnified view of Magnaplate HCR™ coating.

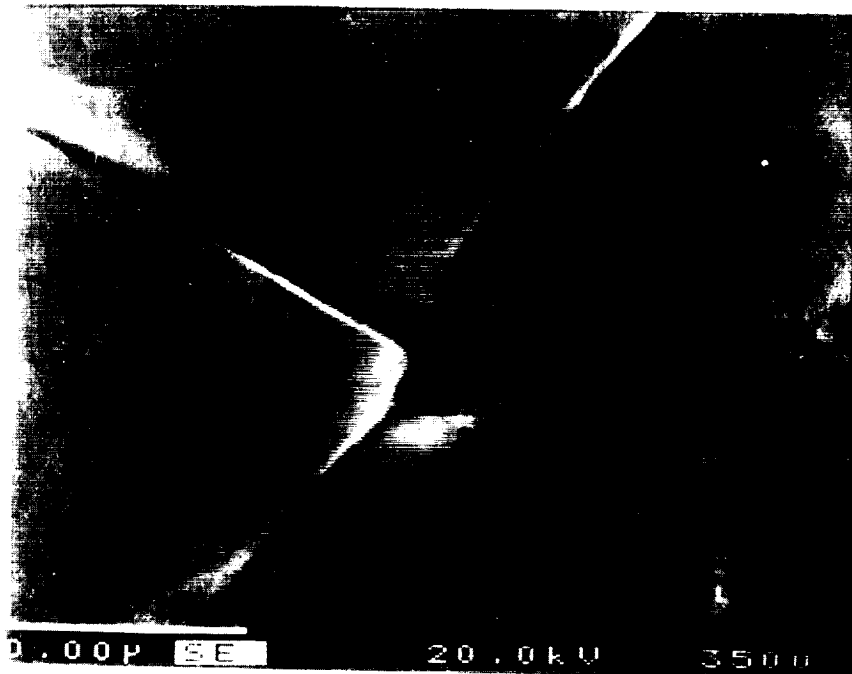


Figure 7. Highly magnified view of Magnaplate HCR™ coating showing tiny cracks.

**2219-T87, 0.3 Mil Coat  
Type II, Class 1  
Water Seal**

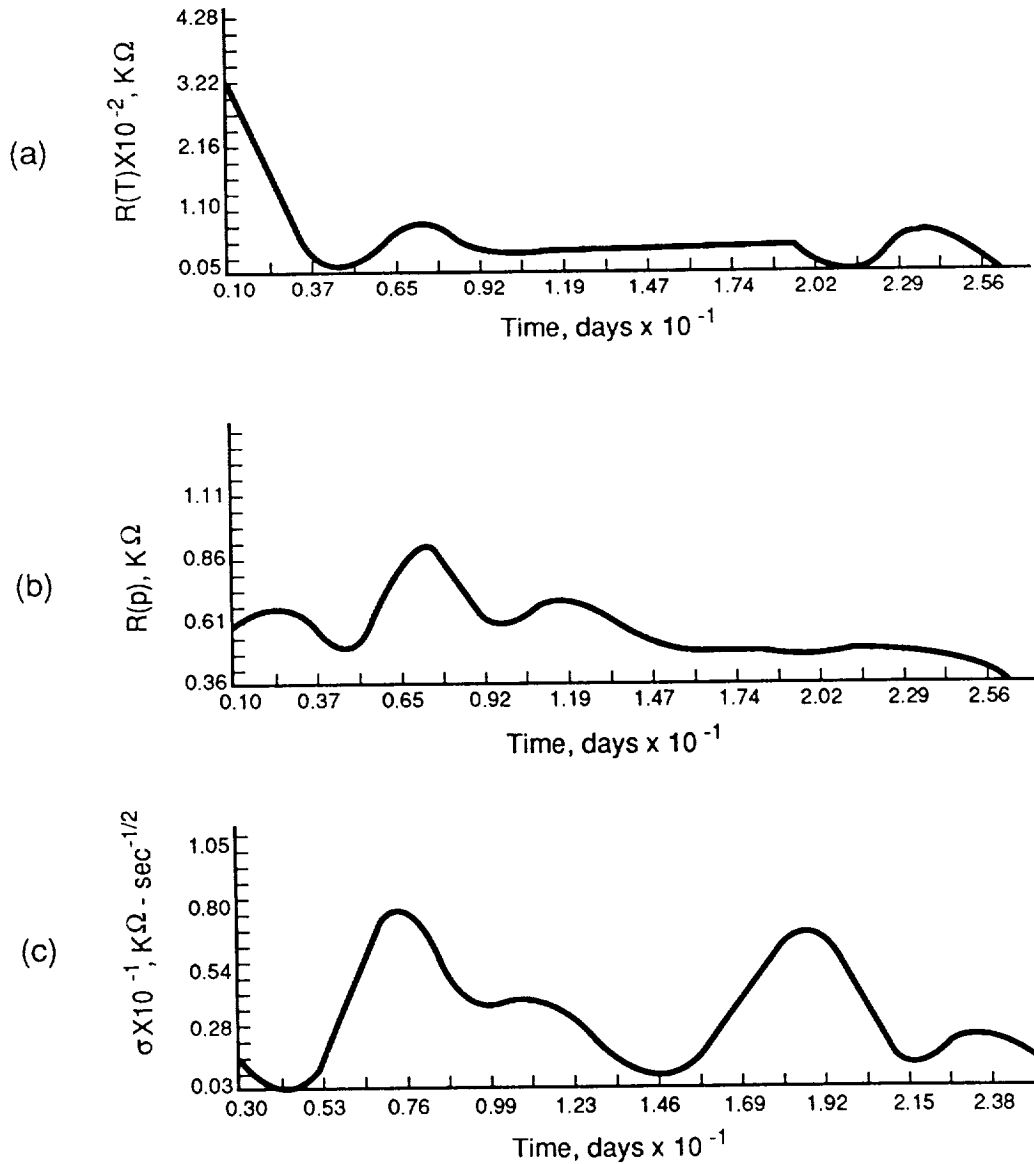


Figure 8.  $R(T)$ ,  $R(P)$ , and Warburg coefficient-time curves for type II anodizing.

**2219-T87, 0.3 Mil Coat  
Type II, Class 1  
Water Seal**

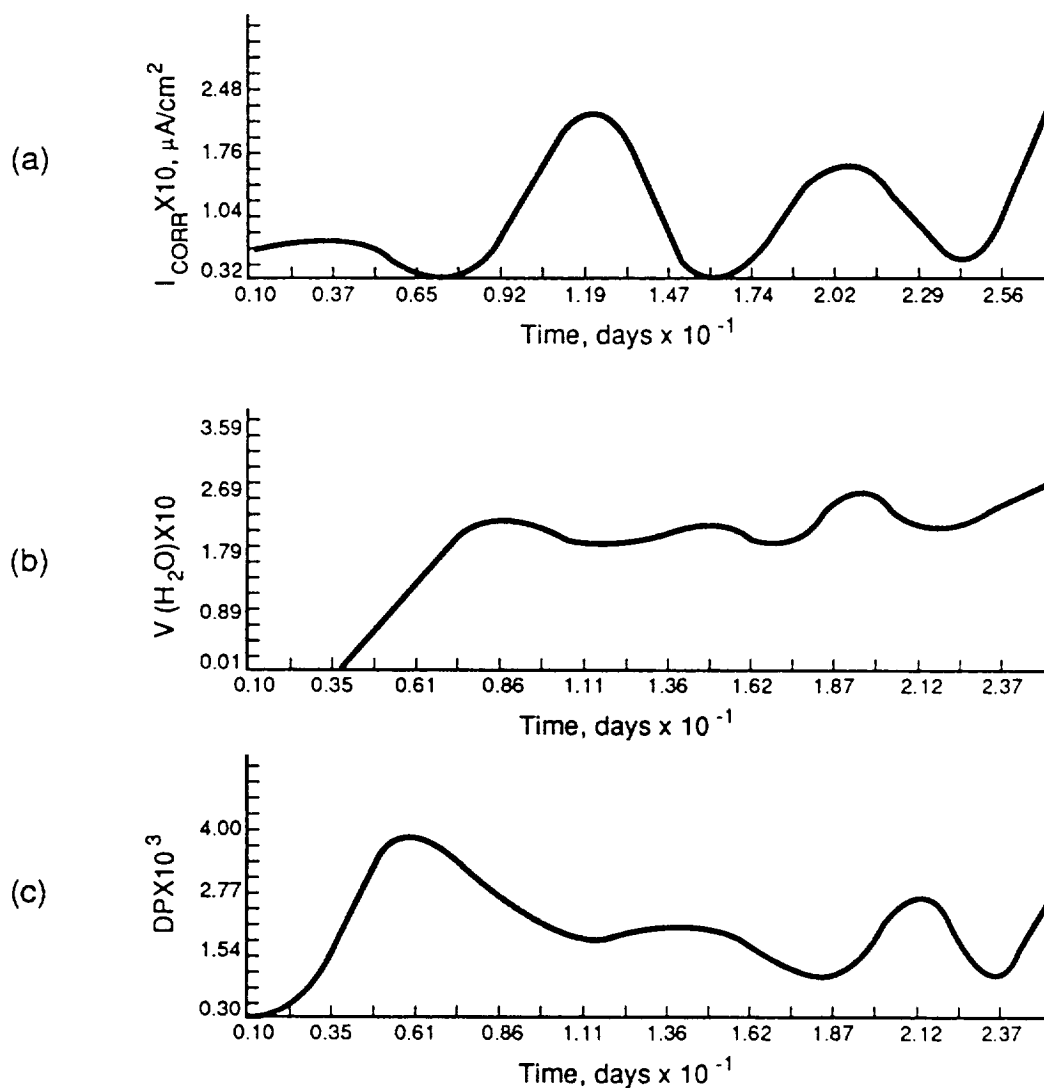


Figure 9.  $I_{CORR}$ , water fraction and delamination-time curves for type II anodizing.

**2219-T87, 0.4 Mil Coat  
Type III, Class 1  
Water Seal**

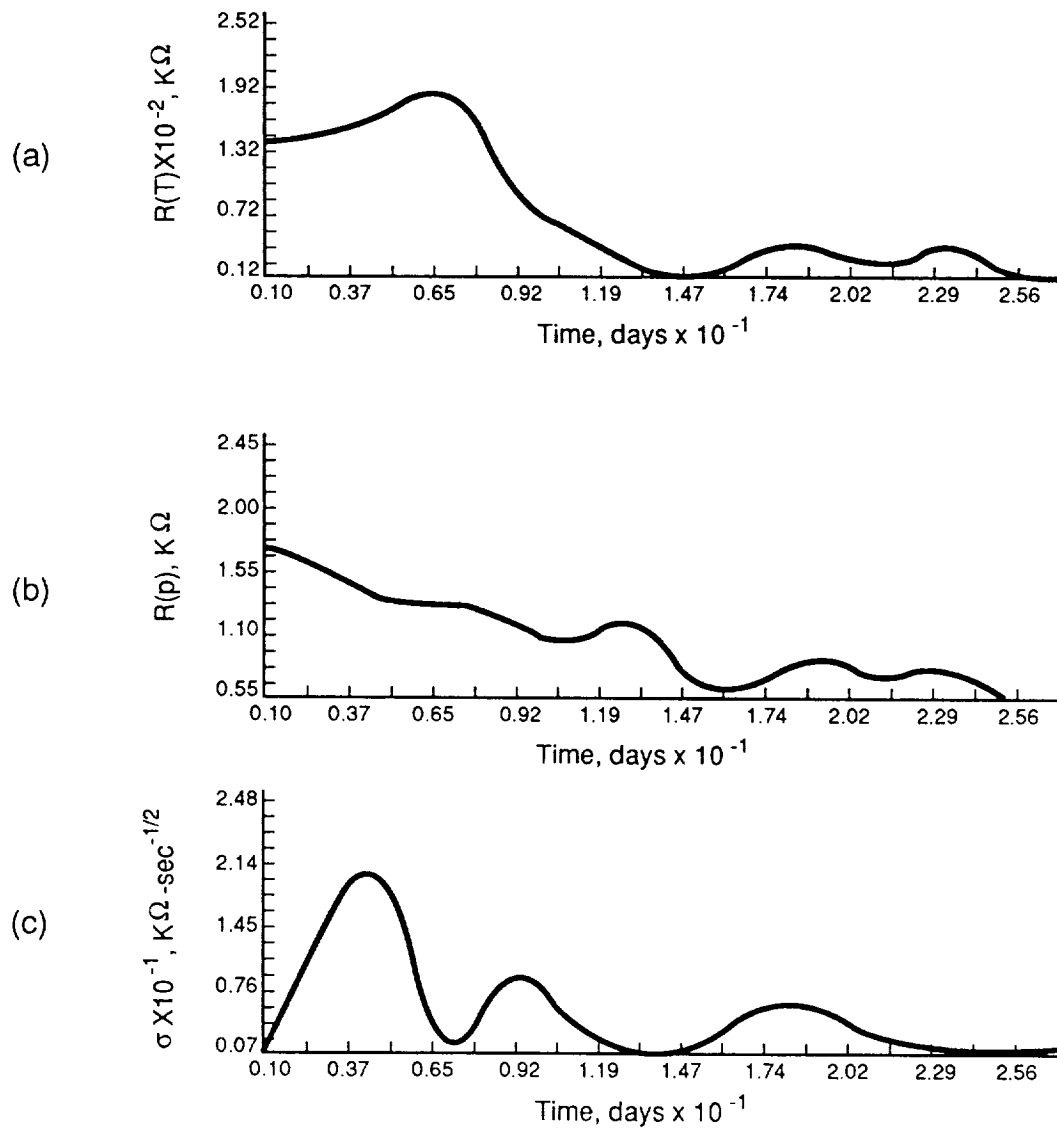


Figure 10.  $R(T)$ ,  $R(P)$ , and Warburg coefficient-time curves for type III anodizing.

**2219-T87, 0.4 Mil Coat  
Type III, Class 1  
Water Seal**

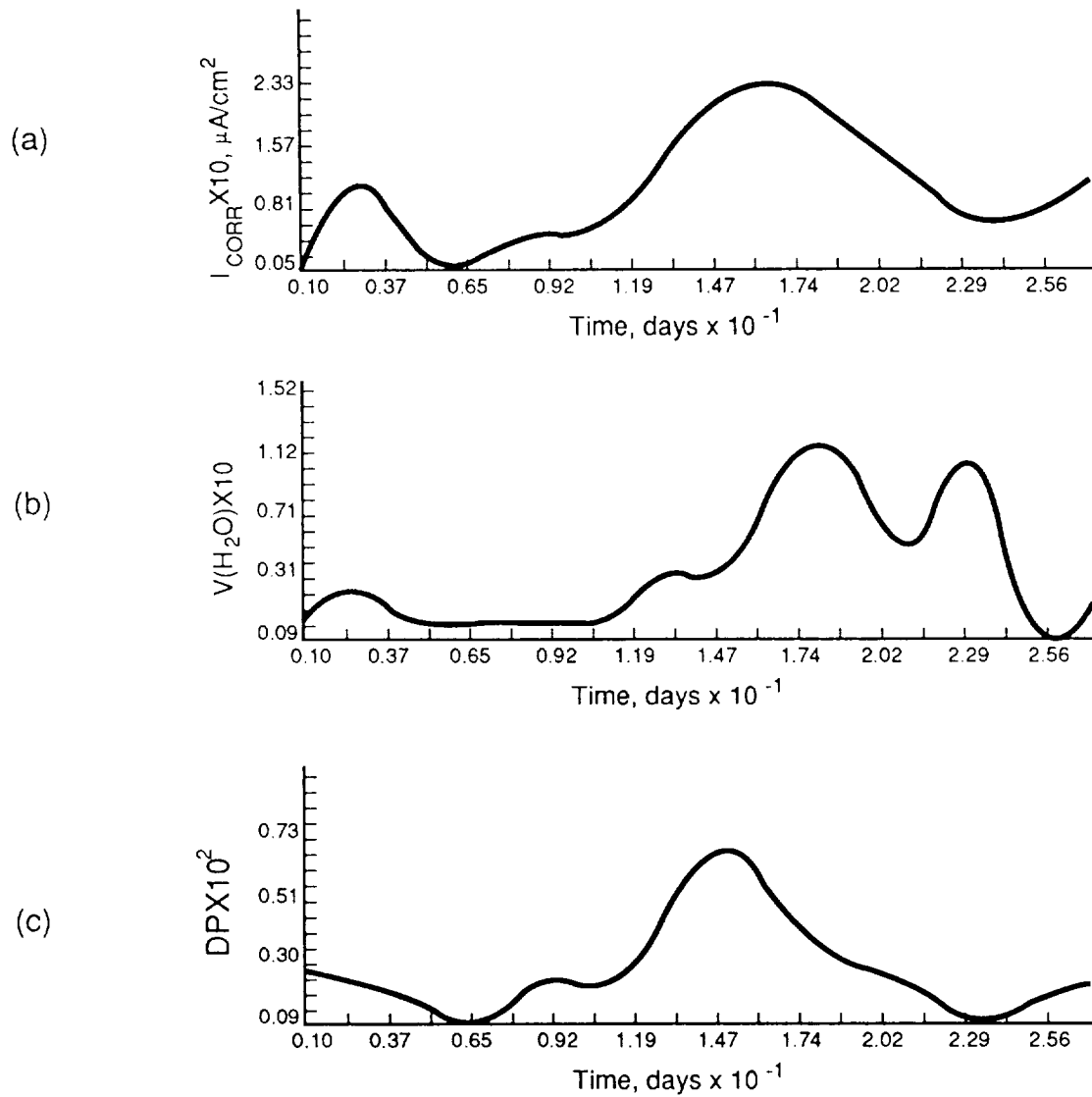


Figure 11.  $I_{CORR}$ , water fraction, and delamination-time curves for type III anodizing.

**2219-T87, 0.2 MIL COAT  
TYPE II, CLASS 1  
WATER SEAL  
pH 5.3**

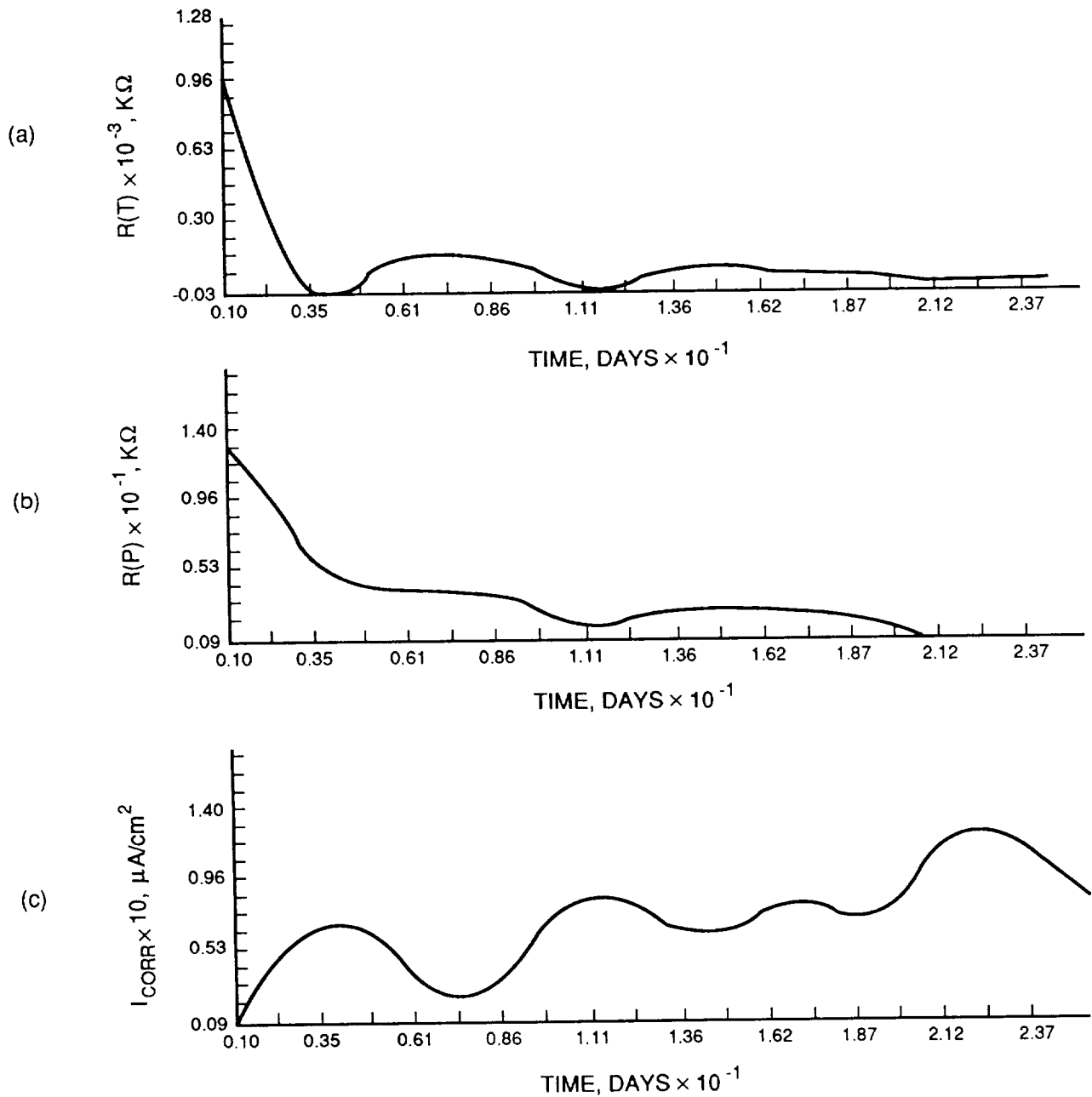


Figure 12.  $R(T)$ ,  $R(P)$ , and  $I_{CORR}$ -time curves for type II anodizing at pH 5.3.

2219-T87, 0.2 MIL COAT  
TYPE II, CLASS 1  
WATER SEAL  
pH 8.8

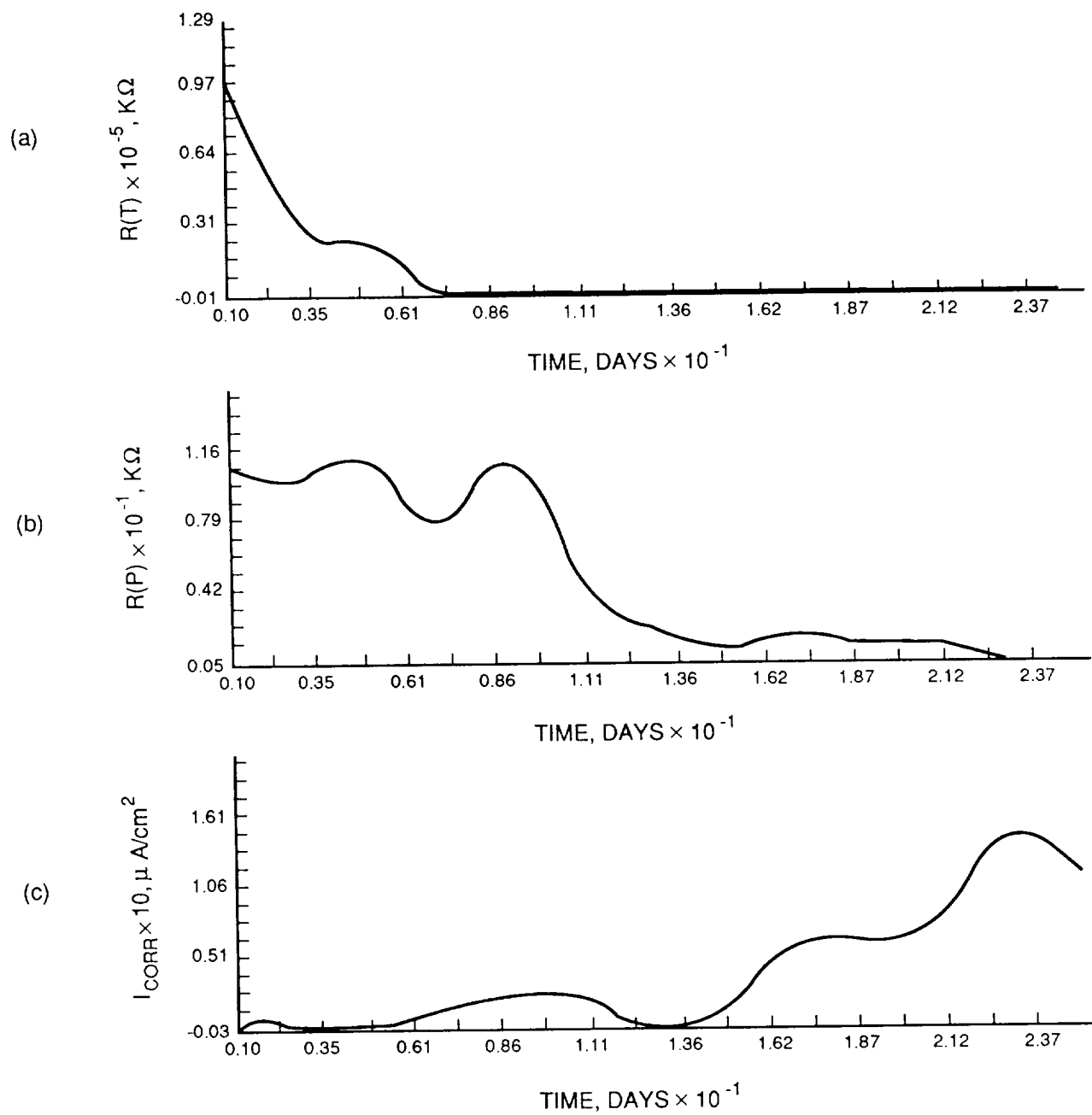


Figure 13.  $R(T)$ ,  $R(P)$ , and  $I_{CORR}$ -time curves for type II anodizing at pH 8.8.

# 2219-T87 ALUMINUM MAGNAPLATE HCR pH 5.5

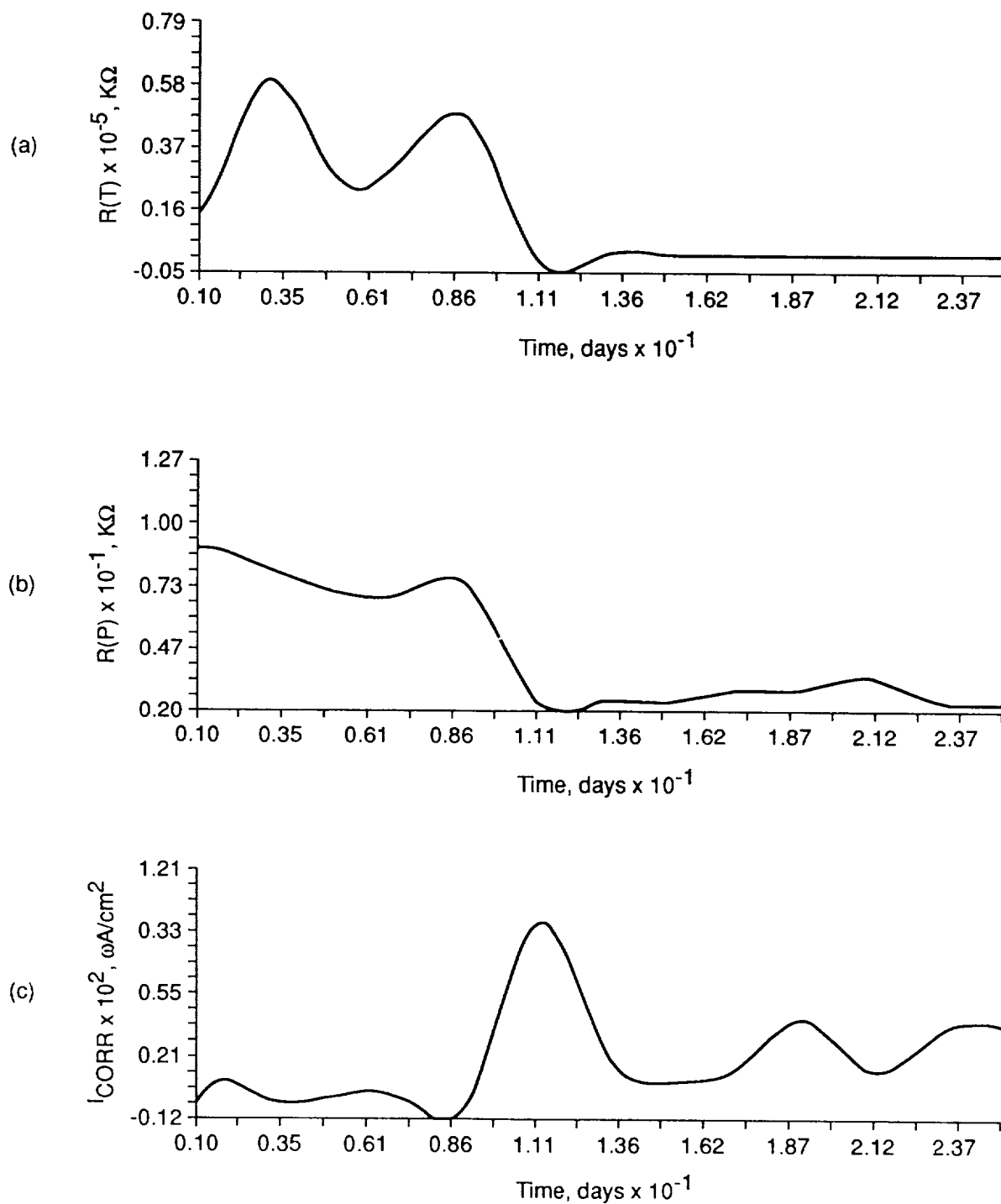


Figure 14.  $R(T)$ ,  $R(P)$ , and  $I_{CORR}$ -time curves for Magnaplate HCR™ coat at pH 5.5.



# 2219-T87 ALUMINUM MAGNAPLATE HCR pH 8.9

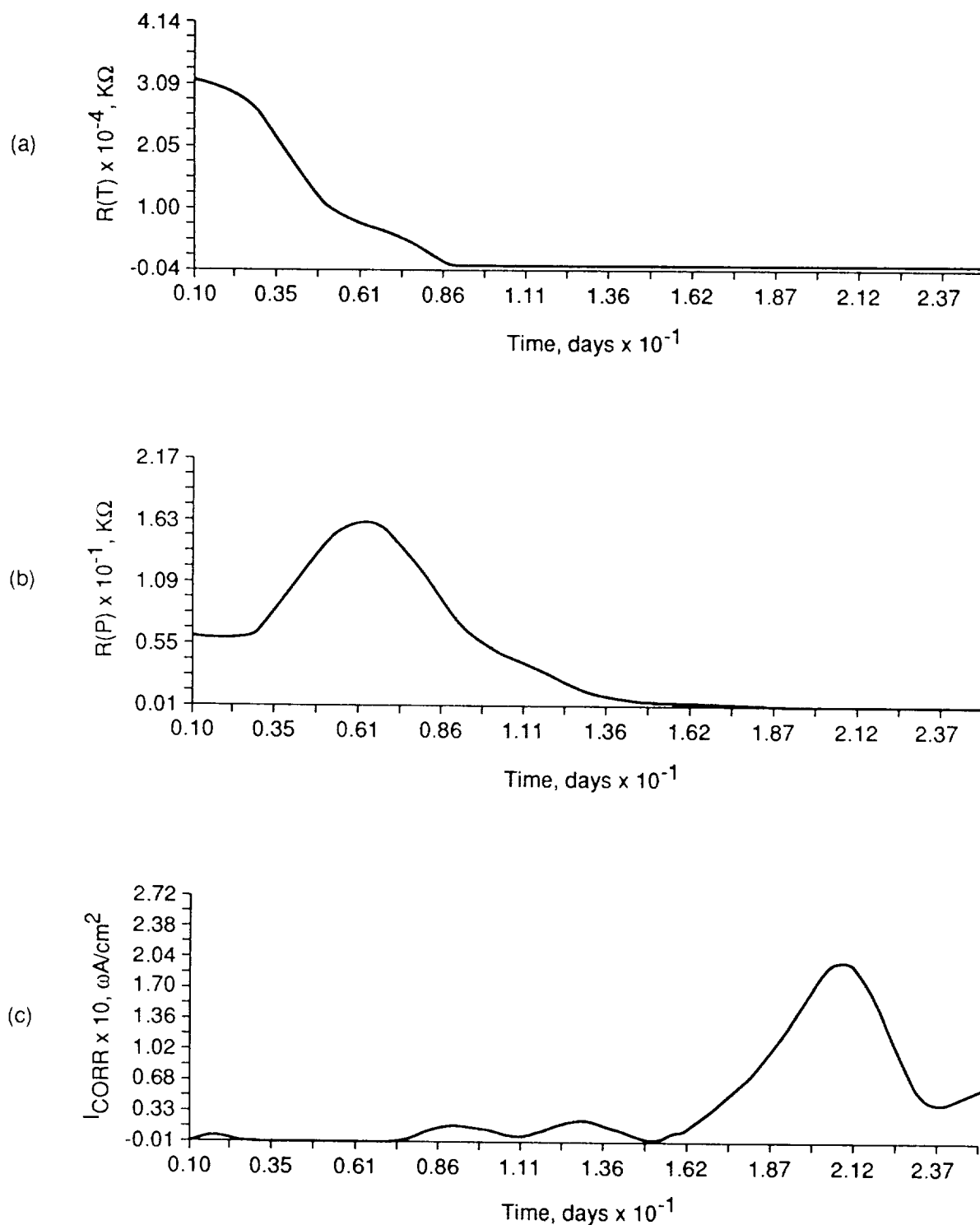


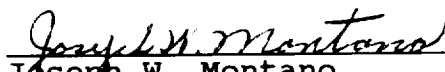
Figure 15.  $R(T)$ ,  $R(P)$ , and  $I_{CORR}$ -time curves for Magnaplate HCR™ coat at pH 8.9.


APPROVAL

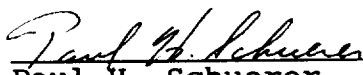
THE CORROSION PROTECTION OF 2219-T87 ALUMINUM BY ANODIZING

By M. D. Danford

The information in this report has been reviewed for technical content. Review of any information concerning Department of Defense or nuclear energy activities or programs has been made by the MSFC Security Classification Officer. This report, in its entirety, has been determined to be unclassified.

  
Joseph W. Montano  
Chief  
Corrosion Research Branch

  
Paul M. Munafo  
Chief  
Metallic Materials Division

  
Paul H. Schuerer  
Director  
Materials & Processes Laboratory